GPS Satellite Observations of a Radiation Belt Dropout Event in the Post-RBSP Era

Alexis Hensley[1], Harriet George[2], David Malaspina [2,3], Milla Kalliokoski[4]

[1] *Berea College, KY, USA,* [2] *Laboratory for Atmospheric and Space Physics (LASP), University of Colorado Boulder, USA,*
[3] *Astrophysical and Planetary Sciences Department, University of Colorado Boulder, USA,* [4] *Japan Aerospace Exploration Agency, JAXA ISAS, Japan*

hensleya2@berea.edu

1. Why use GPS satellite data?

The Earth's radiation belts present a space weather hazard to satellites and astronauts in orbit. The gold-standard radiation belt observations were provided by the Van Allen Probes from 2012 to 2018. **We demonstrated the use of the Global Position System (GPS) satellite data to investigate a radiation belt dropout event, thus examining the feasibility of using GPS satellites to continue to monitor the radiation belts in a post-RBSP era.**

A dropout of relativistic electrons from Earth's outer radiation belt occurred on 14 May 2019 and was analyzed using the GPS constellation. Most GPS satellites carry a Combined X-Ray Dosimeter (CXD) instrument that provides electron count data. **These count data have been cross-calibrated with RBSP electron flux observations to calculate electron fluxes from the GPS observations.** We analyzed this dropout event using electron flux data provided by 19 different GPS satellites to investigate the driving mechanism and timescales of the losses.

2. GPS satellite electron flux data

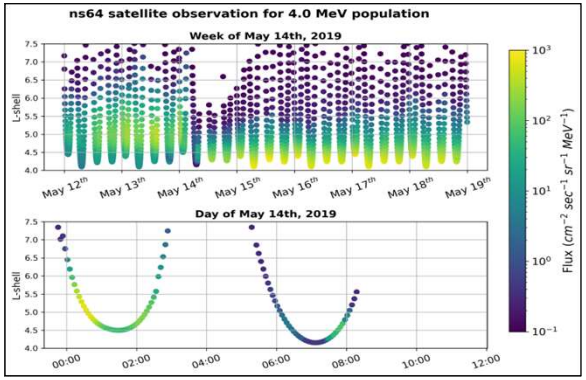

Fig. 1a. *Example of a week's worth of GPS satellite electron flux data observed by the ns64 satellite .* ***Fig. 1b.*** *The same satellite electron flux observations, but focused within 12 hours of the dropout event on May 14th, 2019*

The GPS data provides a **time resolution of 4 minutes**. Therefore, we can observe the dropout in a high-time resolution when combining observations of the 19 satellites. As pictured in the **Fig. 1b.** , we can examine one satellite orbit's electron flux evolution through L-shell of 4 to 7 to a high-degree during the dropout event.

3. Radiation belt dropout event on May 14th, 2019

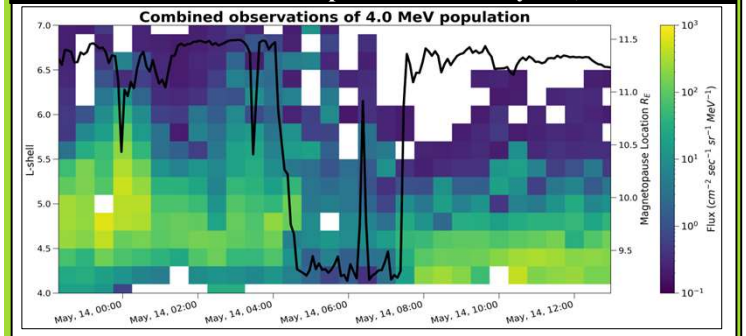

Fig. 2. *Combined flux observations for all 19 satellites within the 12 hours of the event for the 4.0 MeV population. The magnetopause location is displayed atop the flux in order to see the depletion in fluxes in comparison to the magnetopause location.*

4. Solar wind driving conditions

The driving conditions of the dropout event in **Fig. 3.** show a strongly southward IMF during the peak of a high-speed solar wind stream, therefore compressing the magnetopause by ~ 2 R_E for ~ 4 hours. The timing of the magnetopause compression closely corresponds to the time the GPS observed **(e.g. Fig 2**) the dropout event, thus **indicating loss due to magnetopause shadowing**.

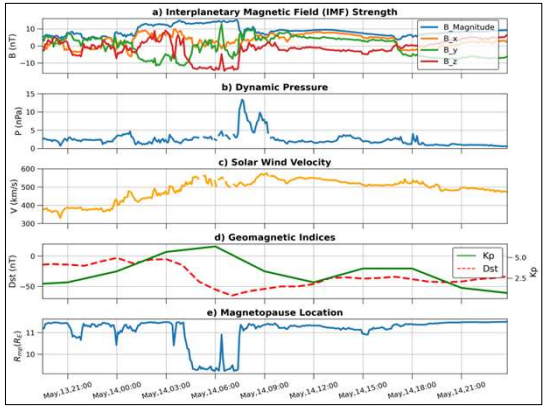

Fig. 3. *Solar wind driving conditions 24 hours within the event from the WIND satellite and accessed through NASA's OMNI website.* ***Fig. 3a.*** *IMF field strength from solar wind data and its components.* ***Fig. 3b.*** *Dynamic pressure from solar wind data.* ***Fig. 3c.*** *Solar wind velocity from solar wind data.* ***Fig. 3d.*** *Planetary index (Kp) and disturbance storm time (Dst) index from online geomagnetic indices.* ***Fig. 3d.*** *Magnetopause location calculated from Shue 1998 model.*

5. Single satellite observations on May 14th, 2019

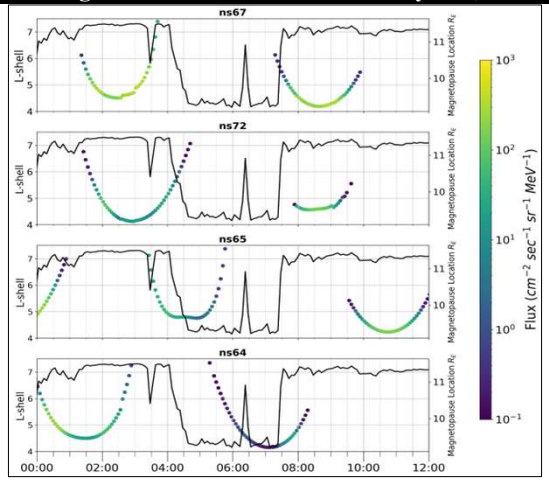

Fig. 4. *Individual satellite observations from 4 of the 19 satellites in order to view different flux observations during the time of the magnetopause compression.*

We can examine the spatial and temporal evolution of the event through the individual observations each satellite offers as they move through the magnetopause location. For example, ns64 shows an immediate recovery of the depleted electron flux as the magnetopause moves outward by ~2 R_E.

6. Phase space density observations on May 14th, 2019

GPS satellites are not equipped with magnetometers, so the **phase space density of the population 3433 MeV /G and 0.11 G$^{1/2}R_E$** was calculated using omnidirectional flux obtained through the CXD forward model (Morley et al. 2016), the TS04D geomagnetic field model (Tsyganenko 2005), and the relativistic electron pitch angle distribution (REPAD) model (Chen et. Al 2014).

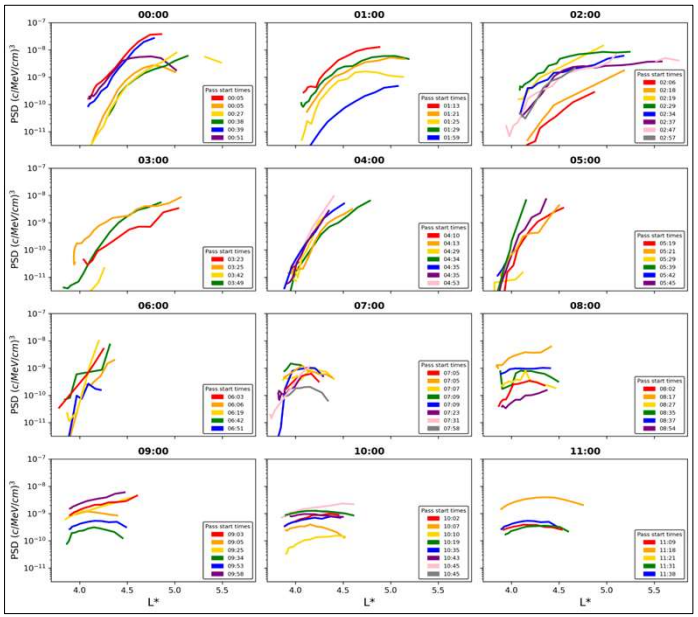

Fig. 5. *The phase space density (PSD) of the 19 satellites inbound and outbound starting passes over an hour within the first 12 hours of May 14th, 2019, in order to see PSD evolution throughout the dropout event.*

Through the phase space density (PSD) evolution we can see the loss from the magnetopause shadowing event within the first 4 hours, but we continue to see loss through the population as **outward radial diffusion acts to transport particles across the magnetopause** therefore flattening the PSD gradient throughout the next couple of hours.

7. Discussion and future work

Electron flux losses of an order of magnitude were observed at all evaluated L-shell in the 4 MeV population. These flux losses were rapid and closely corresponded with a strong compression of the magnetopause. The magnetopause was abruptly compressed from its nominal location by ~ 2 R_E, with the inward incursion starting at approximately 4 AM. Analysis of the phase space density (PSD) showed a total loss of the population between the inward pass of ns65 satellite at 3:20 AM and its outbound at 4:50 AM at all L*> 4.5 R_E. Further examination of the PSD revealed that radial diffusion transported particles across the magnetopause after the initial compression, further contributing to the dropout event,. **This analysis demonstrates the feasibility of using GPS data to evaluate rapid changes in the radiation belts that occurred on timescales of minutes.**

In the future, we are going to continue to investigate the feasibility of Magnetic Local Time (MLT) dependence and calculate the timescale of loss and enhancement of electron populations within the outer radiation belt using GPS satellite data.

References

Chen, Y., Friedel, R. H. W., Henderson, M. G., Claudepierre, S. G., Morley, S. K., and Spence, H. (2014), REPAD: An empirical model of pitch angle distributions for energetic electrons in the Earth's outer radiation belt, *J. Geophys. Res. Space Physics*, 119, 1693– 1708.
Morley, S. K., Sullivan, J. P., Henderson, M. G., Blake, J. B., and Baker, D. N. (2016), The Global Positioning System constellation as a space weather monitor: Comparison of electron measurements with Van Allen Probes data, *Space Weather*, 14, 76– 92.
Tsyganenko, N. A., and Sitnov, M. I. (2005), Modeling the dynamics of the inner magnetosphere during strong geomagnetic storms, *J. Geophys. Res.*, 110, A03208.

Acknowledgments

Thanks to the CXD instrumentation team at Los Alamos National Laboratory!
This research was supported by the National Science Foundation REU program, Award #1950911.